

# Radiation Effects On Exterior Surfaces

**Kehrer Manfred, Dipl.-Ing.,**  
*Hygrothermics Department, Fraunhofer IBP;*  
*Manfred.Kehrer@ibp.fraunhofer.de*

**Schmidt Thomas, Dipl.-Phys.,**  
*Hygrothermics Department, Fraunhofer IBP;*  
*Thomas.Schmidt@ibp.fraunhofer.de*

**KEYWORDS:** *Hygrothermal simulation, radiation, long-wave radiation, radiation model, exterior surface, surface temperature, water content.*

## SUMMARY:

*In hygrothermal simulations usually the long-wave radiation effects are ignored or treated in a simplified way. Temperatures at exterior surfaces can not be calculated accurately in that way. A detailed radiation model has been developed to simulate the hygrothermal behaviour at the exterior surface of building components. Multiple experimental validation calculations show the capability of that model. Furthermore it is shown that neglecting the long-wave radiation effects on exterior surfaces can lead to simulation results which are not “on the safe side”.*

## 1. Introduction

Temperatures at exterior surfaces of building components are affected by heat fluxes in various ways. Beside heat fluxes due to heat conduction within the component and convective heat exchange with the surrounding air radiation effects play a decisive role. Usually only the short wave solar radiation heating up the surface during the day is taken into account explicitly. The long wave, thermal radiation exchange between the exterior surface and the surroundings is often neglected or only modelled with a constant overall increase of the heat transfer coefficient as for instance in a German standard (EN ISO 6946, 1996). Most hygrothermal simulation tools use this simplified model. The real temperatures at surfaces can only be reproduced with limited accuracy in this way. Especially overcooling in the night-time of sky-oriented exterior surfaces below the temperature of the surrounding air can not be calculated. To estimate the risk of algae growth due to temperatures below dew point and water condensation, the effect of thermal emission must be taken into account. An investigation reported in (Energy Design Update, 2006) speculates that in specific climatic zones flat roofs begin to accumulate water if these effects are ignored in their design.

## 2. Radiation Model

In order to accurately calculate the temperatures of exterior surfaces a detailed radiation model was developed at Fraunhofer IBP based on physical fundamentals. This model was integrated into well established hygrothermal software (Künzel, H.M., 1995) for the calculation of the coupled heat and moisture transport in building components.

To quantify all relevant radiation terms affecting an exterior surface a complete balance of all these terms is set up:

$$I = a \cdot I_s + \varepsilon \cdot I_l - I_e \quad (1)$$

$I$	[W/m <sup>2</sup> ]	balanced net radiation at the component's surface
$a$	[-]	short wave absorption coefficient of the component's surface
$I_s$	[W/m <sup>2</sup> ]	short wave solar radiation incident onto the component's surface
$\varepsilon$	[-]	long wave emission coefficient (=absorption coefficient) of the component's surface
$I_l$	[W/m <sup>2</sup> ]	long wave radiation incident onto the component's surface
$I_e$	[W/m <sup>2</sup> ]	long wave radiation emitted by the component's surface

A positive value of the balanced net radiation  $I$  will then lead to a heating up of the component's surface and a negative value will lead to a cooling off. The solar radiation  $I_s$  and the long wave radiation  $I_l$  can be splitted as follows:

$$I_s = I_{s,dir.} + g_{atm.} \cdot I_{s,diff.} + g_{terr.} \cdot I_{s,refl.} \quad (2)$$

$I_{s,dir.}$  [W/m<sup>2</sup>] direct solar radiation  
 $g_{atm.}$  [-] atmospheric field-of-view fraction (atm. FoV)  
 $I_{s,diff.}$  [W/m<sup>2</sup>] diffuse solar radiation  
 $g_{terr.}$  [-] terrestrial field-of-view fraction (terr. FoV)  
 $I_{s,refl.}$  [W/m<sup>2</sup>] solar radiation reflected by the ground

$$I_l = g_{atm.} \cdot I_{l,atm.} + g_{terr.} \cdot (I_{l,terr.} + I_{l,refl.}) \quad (3)$$

$I_{l,atm.}$  [W/m<sup>2</sup>] atmospheric long-wave counterradiation  
 $I_{l,terr.}$  [W/m<sup>2</sup>] terrestrial long-wave counterradiation  
 $I_{l,refl.}$  [W/m<sup>2</sup>] atmospheric long-wave counterradiation reflected by the ground

The two field-of-view fractions are calculated (see DIN EN ISO 6946, 1996) as follows:

$$g_{atm.} = \cos^2\left(\frac{\beta}{2}\right) \quad (4)$$

$\beta$  [°] inclination of the component (90° for a vertical wall)

and

$$g_{terr.} = 1 - g_{atm.} \quad (5)$$

Figure 1 shows the radiative situation of an exterior wall where all radiation terms can be seen.

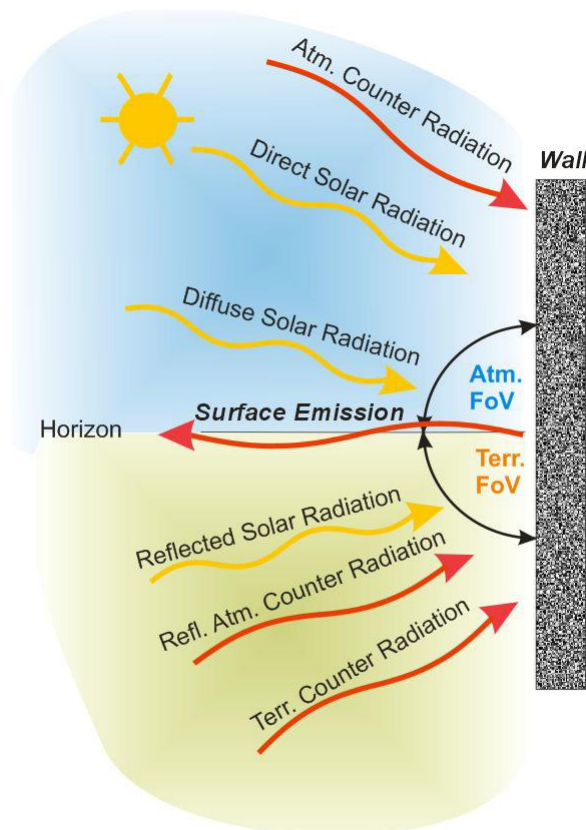


FIG. 1: Radiative situation of an exterior wall.

The equations (2) and (3) contain 3 radiation terms each that we need to know (in hourly values if possible). On the other hand most climatic data sets available typically contain only:

$I_{s,diff.}$	[W/m <sup>2</sup> ]	(see above)
$I_{s,dir.,h.}$	[W/m <sup>2</sup> ]	direct solar radiation on a horizontal surface
$I_{l,atm.}$	[W/m <sup>2</sup> ]	(see above)

To be able to use those generally available climatic data, the other needed radiation terms can be derived as follows:

$$I_{s,refl.} = \rho_{s,terr.} \cdot (I_{s,dir.,h.} + I_{s,diff.}) \quad (6)$$

$\rho_{s,terr.}$  [-] short wave reflection coefficient of the ground

$$I_{l,terr.} = \varepsilon_{l,terr.} \cdot \sigma \cdot T_{terr.}^4 \quad (7)$$

$\sigma$  [W/m<sup>2</sup>K<sup>4</sup>] Stefan-Boltzmann constant (5,67·10<sup>-8</sup>)

$\varepsilon_{l,terr.}$  [-] long wave emission coefficient of the ground

$T_{terr.}$  [K] temperature of the ground

$$I_{l,refl.} = \rho_{l,terr.} \cdot I_{l,atm.} \quad (8)$$

$\rho_{l,terr.}$  [-] long wave reflection coefficient of the ground

The temperature of the ground is set to the air temperature as an approximation, because the ground temperature itself is usually not available.  $I_{s,dir.}$  can be calculated from  $I_{s,dir.,h.}$  as described in (VDI-Guideline 3789, 1994) if the position of the sun is known.

So far, all mentioned radiation terms are explicitly known before the calculation and do not depend on unknown calculation results. In contrast the last radiation term, the long-wave emission from the component's surface, depends on the temperature of the component's surface as follows:

$$I_e = \varepsilon \cdot \sigma \cdot T_{Sur}^4 \quad (9)$$

$T_{Sur}$  [K] temperature of the component's surface

To solve this nonlinear dependency in a linear equation system, as used in our hygrothermal software, equation (9) must be linearized by using a Taylor series. This leads to the following linearized term which can be added to the linear equation system.

$$I_{e,lin} = \varepsilon \sigma T_0^4 + 4 \varepsilon \sigma T_0^3 \cdot (T - T_0) \quad (10)$$

$I_{e,lin}$  [W/m<sup>2</sup>] linearized emitted radiation

$T_0$  [K] temperature of the component's surface before an iteration step

$T$  [K] implicit temperature of the component's surface after the iteration step

### 3. Validation

The validation of the model above is split into two parts. Part No.1 will validate the calculation of the surface temperature if the short-wave and long-wave radiation onto the surface are well known because they have been measured. Part No. 2 will validate the calculation of the long-wave radiation incident onto the surface from the climatic data typically available.

#### 3.1 Calculation of the surface temperature

For this validation documented field test at the IBP is used. The considered wall assembly has the following composition starting from the exterior:

light-gray wall colour;

2 mm finishing plaster;

- 3 mm reinforcement plaster;
- 10 cm polystyrene insulation;
- 36,5 cm masonry wall;
- 1 cm gypsum plaster.

Because of the thermal decoupling of the exterior plaster and the small heat capacity of the exterior plaster the temperature at the component's surface is mainly depending on the exterior boundary conditions (temperature and radiation). In addition, the wall is north oriented, therefore night-time overcooling below ambient air temperature is expected. Surface temperature, air temperature, short-wave and long-wave radiation onto the surface ( $I_s$  and  $I_l$ ) have been measured. Also the RH of the air was measured at the IBP weather station nearby. The long-wave and short-wave absorptivity ( $a=0.39$ ;  $\varepsilon=0.96$ ) were measured at the IBP laboratory. A convective heat transfer coefficient of  $8 \text{ W/m}^2\text{K}$  was used which corresponds roughly to a mean air speed of  $1 \text{ m/s}$  during the investigated time period (see EN ISO 6946, 1996).

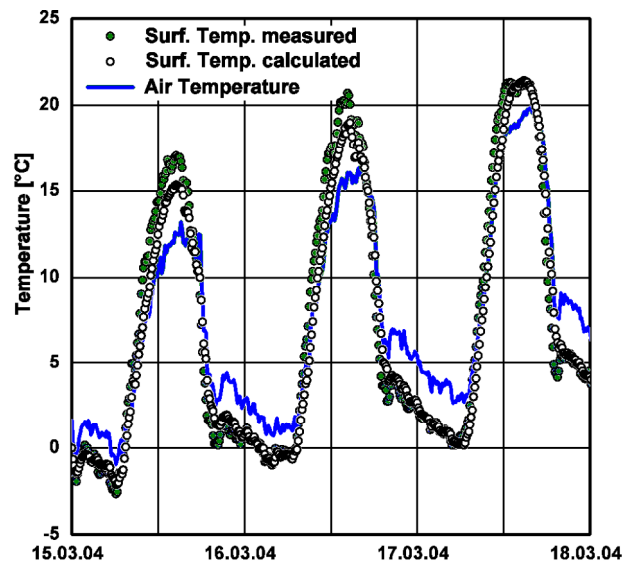


FIG. 2: Measured and calculated surface temperatures at IBP test site.

Figure 2 shows the comparison of measured and calculated temperatures at the surface of the EIFS wall at the IBP test site during a period of three days. We can see a maximum deviation of about  $2 \text{ }^\circ\text{C}$  between measured and calculated temperatures by day. In particular, we notice good agreement of both temperatures by night. The overcooling effect is represented very well and one should notice that the calculated surface temperatures would not fall at all below the ambient air temperature if these long-wave radiation effects were just modelled with an overall increase of the heat transfer coefficient.

### 3.2 Calculation of the long-wave radiation incident onto the surface

To validate equation (3) we use the measured values of two pyrgeometers at the IBP test site which have a wavelength range from  $5 \text{ } \mu\text{m}$  to  $25 \text{ } \mu\text{m}$  (see Figure 3). We use the measured long-wave radiation data  $I_{l,am}$  of the horizontal pyrgeometer and calculate the long-wave radiation  $I_l$  expected on a vertical wall. For this we need the air temperature taken from the IBP weather station as an approximation for ground temperature. Afterwards we can compare the calculated and the measured long-wave radiation onto a vertical wall (see Figure 4). Hourly values of a three year period are shown in this diagram and every dot represents a one hour value which ideally should be on the bisecting line. We can see generally good agreement, but we also have to notice a systematic difference between measurement and calculation (about  $9 \text{ W/m}^2$ ). The reason for this systematic difference is probably the fact that we assume all parts of the sky to contribute equally to the long-wave radiation measured on the horizontal surface which is only an approximation of the reality. Further investigations will follow.



FIG. 3: Horizontal (left) and vertical (right) pyrometers at the IBP test site.

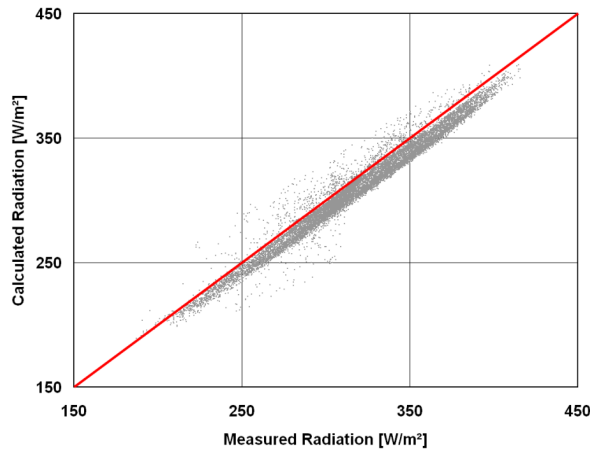


FIG. 4: Comparison of calculated and measured long-wave radiation onto a vertical wall.

#### 4. Application and Conclusion

The following application will show the hygrothermal consequences if the complete radiation model described above is used. Figure 5 shows the assembly and the hygrothermal model of a typical wooden flat roof construction. The exterior bitumen felt is white colored (short-wave absorptivity 0.2; long-wave emissivity 0.9) to protect the roof from solar heat gain in summer. The roof is located in Holzkirchen, Germany and the climate file of 2003 is used where hourly values of  $I_{s,diff}$ ,  $I_{s,dir,h}$  and  $I_{l,atm}$  were measured hourly at the IBP weather station.

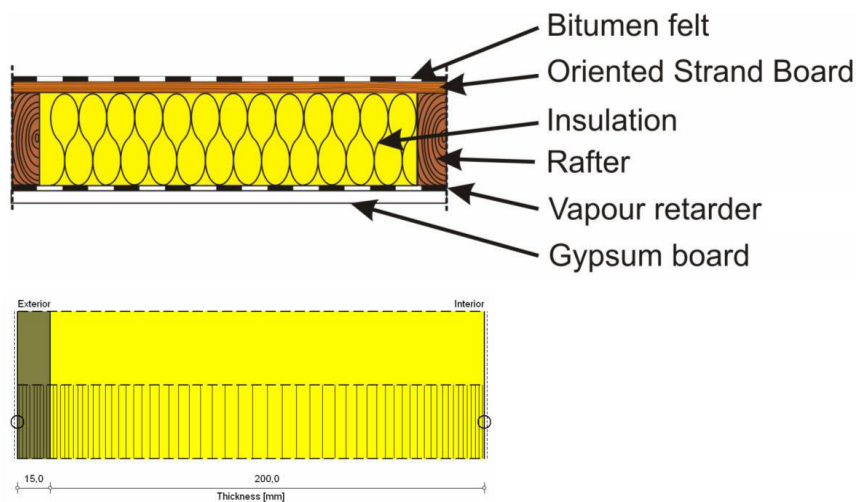


FIG. 5: Assembly (top) and hygrothermal model (bottom) of a typical wooden flat roof construction.

The following three variants were considered:

- simplified long-wave exchange (traditional approach);
- complete radiation balance;
- no solar radiation.

The variant “simplified long-wave exchange” models the long-wave exchange by adding a constant contribution to the heat transfer coefficient. A standard value is used for this constant.

The variant “no solar radiation” uses the simplified long-wave exchange, too, but tries to compensate for the lack of night time overcooling by omitting the drying potential furnished by solar heating. If validated, this approach could be used by simulation tools with simplified radiation models to obtain nevertheless results “on the safe side”.

The water content of the OSB board in all three variants can be seen in Figure 6. The variant “simplified long-wave exchange” shows a decreasing water content of the OSB board. This could lead to the mistaken conclusion that the construction performs well. In contrast the variant “complete radiation balance” shows that moisture damage will most likely occur, because of the accumulation of water within the OSB board. Also, the variant “no solar radiation” has an increasing water content and will lead to the conclusion that this is a problematic construction. But the moisture accumulation is not as large as in the variant “complete radiation balance”. Therefore we should notice that neglecting solar radiation effects on the exterior surface need not to produce results which are “on the safe side”, if white paint on the exterior surface is used.

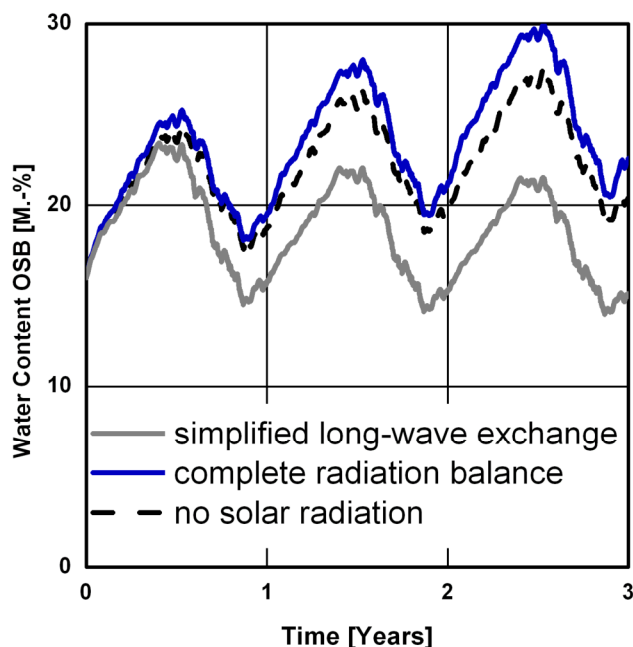


FIG. 6: Water content within the OSB board of all three variants.

## 5. References

- Energy Design Update® (2006). In Arizona, White Roofing Causes Wet Insulation, Vol. 26, No. 6, S. 4-6, Aspen Publishers.
- EN ISO 6946 (Nov. 1996). Bauteile – Wärmedurchlasswiderstand und Wärmedurchgangskoeffizient – Berechnungsverfahren.
- Künzel H.M. (1995). Simultaneous Heat and Moisture Transport in Building Components. - One- and two-dimensional calculation using simple parameters, University Stuttgart, IRB Verlag.
- VDI-Guideline 3789 (1994). Umweltmeteorologie – Wechselwirkungen zwischen Atmosphäre und Oberflächen. Berechnung der kurz- und langwelligen Strahlung.